

Double-slit Fraunhofer pattern as the signature of the Josephson effect between Berezinskii superconductors through the ferromagnetic vortex.

M.A. Silaev¹

¹*Department of Physics and Nanoscience Center, University of Jyväskylä,
P.O. Box 35 (YFL), FI-40014 University of Jyväskylä, Finland*

(Dated: September 11, 2017)

I apply the recently developed formalism of generalized quasiclassical theory to show that using hybrid superconducting systems with non-collinear strong ferromagnets one can realize the Josephson junction between Berezinskii-type superconductors. The reported calculation reproduces main features observed in the recent experiment, namely the the slightly asymmetric double-slit Fraunhofer interference pattern of the Josephson current through the ferromagnetic vortex. The double-slit structure results from the spatially inhomogeneous Berezinskii state with the amplitude controlled by the local angle between magnetic moments in two ferromagnetic layers. The critical current asymmetry by the sign of magnetic field can signal the presence of spontaneous supercurrents generated by the non-coplanar magnetic texture near the core of the ferromagnetic vortex core. I demonstrate that ferromagnetic vortex can induce spontaneous vorticity in the odd-frequency order parameter manifesting the possibility of the emergent magnetic field to create topological defects.

During the recent years large attention has been devoted to the studies of long-range proximity effect and spin-polarized Josephson currents carried by the spin-triplet Cooper pairs in superconductor/ferromagnet/superconductor (S/F/S) heterostructures¹⁻⁴. This interest is motivated the possible applications of spin-polarized superconducting currents in spintronics. Much effort is invested to the studies of tunable spintronic elements where the Josephson current⁵⁻¹³ or the critical temperature¹⁴⁻¹⁹ are controllable by the magnetic degrees of freedom. One of the possible ways for the implementation of such a device has been suggested in my work²⁰ employing the well-controlled properties of the nanomagnets with vortex-like magnetization patterns. In that proposal I have demonstrated that it is possible to gain the effective control over the long-range proximity effect by tuning the position of ferromagnetic (FM) vortex with the help of external in-plane magnetic field.

Recently the conceptually similar device has been realized experimentally²¹. Schematically this system is shown in the Fig.(1)a. It consists of two spin-textured ferromagnets F and F' with the magnetizations \mathbf{M} and \mathbf{M}' and the superconducting layer S. The thin layer F' is in the contact with superconductor and contains a gap. The Josephson current flows through the layer F which contains FM vortex. It has been observed that the presence of FM vortex in the system results in the non-trivial modification of the critical current dependence $I_c = I_c(H)$ as a function of the external magnetic field H . The striking features produced by the FM vortex is that this dependence becomes similar to the double-slit Fraunhofer interference pattern instead of the usual single-slit form produces by the homogeneous junction.

I demonstrate below that this behaviour can be considered as the direct experimental signatures of the Josephson effect between Berezinskii-type superconductors characterized by the spin-triplet odd-frequency s-wave order parameters²²⁻²⁹. Such superconducting state

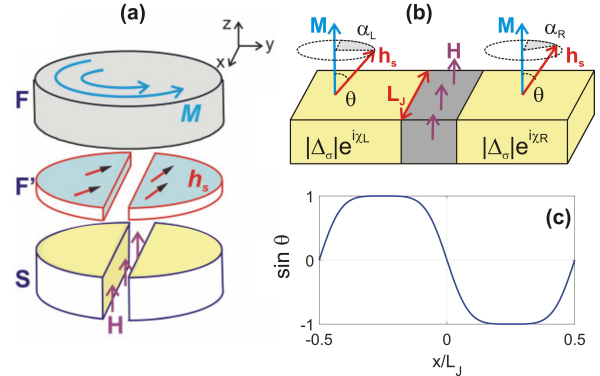


FIG. 1. (Color online) (a) Geometry of the Josephson S/F'/F device with FM vortex in the F layer and the in-plane magnetic texture in the F' layer. (b) Model of the non-homogeneous Josephson junction with usual $\Delta\chi = \chi_R - \chi_L$, spin-dependent $\Delta\alpha = \alpha_R - \alpha_L$ phase differences and the texture of the angle $\theta = \theta(x)$ between \mathbf{M} and $\mathbf{h}_s \parallel \mathbf{M}'$. (c) Model dependence of $\sin\theta(x)$ near the junction.

is induced in the F layer in result of the combined effect of Zeeman splitting in the S electrode and filtering of equal-spin (ES) Cooper pairs in F. Qualitatively the unusual Fraunhofer patterns are explained by the intrinsic inhomogeneity of the induced Berezinskii state which depends on the relative orientation of the local magnetic moments in F and F' layers, \mathbf{M} and \mathbf{M}' respectively. The amplitude of induced order parameter is defined by the polar angle θ between \mathbf{M} and \mathbf{M}' , see Fig.1b. The variation of $\theta = \theta(x)$ resulting from the magnetic texture along the junction leads to the the experimentally observed double-slit pattern of the critical current²¹. Besides that, the azimuthal angle α produces spin-dependent phases of the order parameter components. The variation of α arises in non-coplanar magnetic textures and in strong ferromagnets with lifted spin degeneracy it produces spontaneous supercurrents³⁰⁻³⁵. The spatial dependence of $\alpha = \alpha(x)$

along the junction is therefore equivalent to the emergent localized magnetic field and results in the critical current asymmetry $I_c(H) \neq I_c(-H)$ which can signal the presence of spontaneous supercurrents through the FM vortex.

The system shown in Fig. 1a can be described analytically using several assumptions. First, the layers are supposed to be thin enough to neglect the variation of magnetization fields along the z coordinate. Next, the layer F' is assumed to induce an effective exchange field within the superconducting electrode $\mathbf{h}_s \parallel \mathbf{M}'$. This model is justified by the small thickness of the F' layer which allows to neglect the variation of correlation functions along z . The Green's functions in F'/S layer can be found considering just the superconducting layer with the thickness-averaged exchange field³⁶ $\mathbf{h}_s = \mathbf{h}_{F'} d_{F'}/(d_{F'} + d_S)$ where $\mathbf{h}_{F'} \parallel \mathbf{M}'$ is the exchange field in F', $d_{F'}$ and d_S are the thickness of the F' and S layers correspondingly. For simplicity the density of states is taken equal in S and F'. This exchange field leads to the significant critical temperature suppression of the S/F'/F structure observed in the experiment²¹. The role of this exchange field is to produce the mixed-spin triplet Cooper pairs which can be converted into the equal-spin correlations (ESC) in the ferromagnetic layer due to the spin-dependent tunnelling^{34,35}.

The F layer hosting FM vortex has rather large thickness as compared to the mean free path, so that only the equal-spin correlations (ESC) residing on separate spin-split Fermi surfaces can penetrate to the full thickness. The generalized Usadel equation describing ESC quasiclassical propagators \hat{g}_σ derived in Ref.⁽³⁵⁾ reads

$$D_\sigma \hat{\partial}(\hat{g}_\sigma \hat{\partial} \hat{g}_\sigma) - [\hat{\Delta}_\sigma + \omega \hat{\tau}_3, \hat{g}_\sigma] = 0 \quad (1)$$

where $\sigma = \pm 1$ is the spin subband index, D_σ are the spin-dependent diffusion coefficients. The covariant differential operator is

$$\hat{\partial}_\mathbf{r} = \nabla_\mathbf{r} + i\sigma \mathbf{Z}[\hat{\tau}_3, \cdot] - ie\mathbf{A}[\hat{\tau}_3, \cdot], \quad (2)$$

where \mathbf{A} is the electromagnetic vector potential, \mathbf{Z} is the adiabatic spin gauge field, and D_σ are the spin-dependent diffusion coefficients. The generalized Usadel equation (1) is supplemented by the expression for the current

$$\mathbf{j} = i\pi T e \sum_{\sigma=\pm} \sum_{\omega} \nu_\sigma D_\sigma \text{Tr}[\tau_3 \hat{g}_\sigma \hat{\partial}_\mathbf{r} \hat{g}_\sigma], \quad (3)$$

where ν_\pm is the spin-up/down density of states (DOS).

The effective spin-dependent order parameter $\hat{\Delta}_\sigma$ in Eq.(1) describing the ES components of the proximity-induced order parameter can be obtained from the non-diagonal part of the general tunnelling self-energy³⁷⁻⁴⁰

$$\hat{\Sigma} = \gamma \hat{\Gamma} \hat{F} \hat{\Gamma}^\dagger, \quad (4)$$

where $\hat{F} = (g_{01}\sigma_0 + g_{31}\boldsymbol{\sigma}\mathbf{n}_h)e^{i\chi\hat{\tau}_3}\hat{\tau}_1$ is the anomalous Green's function in the superconductor with exchange field, $\mathbf{n}_h = \mathbf{h}_s/h_s$. In the absence of spin-orbital relaxation the spin-singlet and spin-triplet parts are given by

$g_{01} = [F_{bc_s}(\omega + ih_s) + F_{bc_s}(\omega - ih_s)]/2$ and $g_{31} = [F_{bc_s}(\omega + ih_s) - F_{bc_s}(\omega - ih_s)]/2$, where $F_{bc_s}(\omega) = \Delta/\sqrt{\omega^2 + \Delta^2}$. The spin-polarized tunnelling matrix has the form $\hat{\Gamma} = t\hat{\sigma}_0\hat{\tau}_0 + u\boldsymbol{\sigma}\mathbf{m}\hat{\tau}_3$ where $\mathbf{m} = \mathbf{M}/M$ is the direction of magnetization in the ferromagnet and $\gamma = \sigma_n R$ is the parameter describing the barrier strength, R is the normal state tunnelling resistance per unit area. The normalized tunnelling coefficients are $t = \sqrt{1 + \sqrt{1 - P^2}}/2$, $u = \sqrt{1 + \sqrt{1 - P^2}}/2$ and P is the effective spin-filtering coefficient that ranges from 0 (no polarization) to 1 (100% filtering efficiency). Then the ES component of the tunnelling self-energy is given by

$$\hat{\Sigma}_{ES} = \gamma g_{31} e^{i\chi\hat{\tau}_3} [\hat{\tau}_1 \boldsymbol{\sigma} \mathbf{h}_s + P \hat{\tau}_2 \boldsymbol{\sigma} (\mathbf{h}_s \times \mathbf{m})]. \quad (5)$$

Projecting $\hat{\Sigma}_{ES}$ to the spin-up and spin-down states with respect to the quantization axis set by the magnetization \mathbf{m} we get the ES components of the effective spin-triplet order parameter

$$\hat{\Delta}_\sigma = h_\perp \Delta_{F\sigma} \tau_1 e^{i\tau_3(\chi + \sigma\alpha)}, \quad (6)$$

with the amplitude given by $\Delta_{F\sigma} = -(1 + \sigma P)g_{31}$ and the prefactor $h_\perp = \sin\theta$ which is the projection of exchange field to the plane perpendicular to the magnetization direction, θ is the polar angle of \mathbf{h}_s in the coordinate system defined by \mathbf{m} . The distribution of $\sin\theta$ can be obtained by the micromagnetic simulations²¹ for the realistic geometry. The additional spin-dependent phase α in Eq.(6) is defined by the azimuthal angle of \mathbf{h}_s as shown in Fig.(1)b. For the in-plane textures when both \mathbf{m} and \mathbf{h}_s lie in the xy plane the additional phase in Eq.(6) is absent $\alpha = 0$. However near FM vortex core the texture becomes non-coplanar which leads to the gradients of α , which are coupled to the spin gauge field^{35,41} \mathbf{Z} so that the combination

$$\mathbf{V}_s = \sigma(\nabla\alpha - 2\mathbf{Z}) \quad (7)$$

has the meaning of the texture-induced part of the superfluid velocity. In strong ferromagnets with broken spin degeneracy \mathbf{V}_s produces spontaneous charge supercurrents^{30,35} resulting in the shift of the Fraunhofer pattern as shown below.

Due to the symmetry $g_{31}(\omega) = -g_{31}(-\omega)$ the pairing amplitude in Eq. (6) represents the odd-frequency spin-triplet s-wave superconducting order parameter suggested by Berezinskii²² and intensively studied afterwards²³⁻²⁹. The odd superconducting correlations has been studied in several setups with proximity-induced superconductivity in ferromagnets^{2,42}, normal metals⁴³⁻⁴⁵, topological insulators^{46,47} and non-equilibrium systems⁴⁸. Usually due to the broken translational or/and spin-rotation symmetries the total Cooper wave function in proximity systems is a superposition of odd- and even- frequency components which inevitably coexist at one and the same point⁴³⁻⁴⁹, except the discrete set of points in the cores of proximity-induced vortices⁵⁰. In contrast, the order parameter in

Eq.(6) represents the pure Berezinskii state without admixtures of spin-singlet and/or even-frequency components. Therefore the setup shown in Fig.(1)a consisting of two non-collinear strong ferromagnets emulates the Josephson effect between two Berezinskii superconductors through the FM vortex. Note that the absence of even-frequency spin-singlet pairings in the Eq.(6) is not exact, since the singlet correlations can strictly speaking penetrate even to the strong ferromagnetic layers. However in the dirty regime the singlet amplitude is exponentially suppressed at distances larger than the mean free path from the F/S interface, so that the presence of such components does not affect transport properties in the thick ferromagnetic layer.

Experimentally the signature of Josephson current between proximity-induced Berezinskii superconductors can be obtained due to the non-trivial structure of the order parameter (6), which amplitude depends on the angle θ between magnetic moments in F and F' layers. Such a dependence is peculiar for the spin-triplet odd-frequency pairings since the spin-singlet component is not sensitive to the exchange field rotations. As shown below, that results in the striking modification of the Fraunhofer pattern in the critical current as a function of external magnetic field $I_c = I_c(H)$ which reflects the inhomogeneity of the magnetic texture in the S/F'/F system. This behaviour coincides qualitatively with recent experimental observations²¹.

The Josephson effect in the setup shown in Fig.(1)a can be analysed using the formalism of Eqs.(1,3,6). Due to the small distance between superconducting electrodes one can use the model 1D system shown in Fig.1b which is the long junction with gap functions in the leads given by (6). There are two key points to understand the experimental results. First, the effective gap amplitude is $\Delta_\sigma \propto \sin \theta$ that is determined by the angle θ between \mathbf{m} and \mathbf{h}_s . As shown by the magnetization pattern data²¹, θ changes quite strongly along the junction both due to the vortex-like pattern in F and the distortions of the monodomain state in F' near the trench that cuts S and F' layers. The model distribution of θ along the Josephson junction that is used in calculations is shown in Fig.1c and described by $\theta(x) = (\pi/2)\tilde{\theta}(x/L_J)$, where

$$\tilde{\theta}(\tilde{x}) = \tanh\left(\frac{\tilde{x}}{w_c}\right) \tanh\left(\frac{\tilde{x} - 0.5}{w_e}\right) \tanh\left(\frac{\tilde{x} + 0.5}{w_e}\right). \quad (8)$$

The basic features of this profile is that $\theta = 0$ at the FM vortex center $x = 0$ and at the edges $x = \pm L_J/2$, while reaching $\pm\pi/2$ at the middle points. The dimensionless widths w_e and w_c determine the shape of the Fraunhofer pattern. Second, near the FM vortex core the magnetization pattern is non-coplanar which generates both the gauge field \mathbf{Z} and the spin-dependent phase $\alpha = \alpha(x)$ distribution along the junction. Using the model magnetization distribution $\mathbf{m} = (m_\perp \cos \varphi, m_\perp \sin \varphi, m_z)$, where φ is the real-space polar angle one obtains $\mathbf{Z} = m_z \nabla \varphi/2$ and $\alpha = \arctan[m_z \tan(\varphi - \varphi_0)]$, where φ_0 is the az-

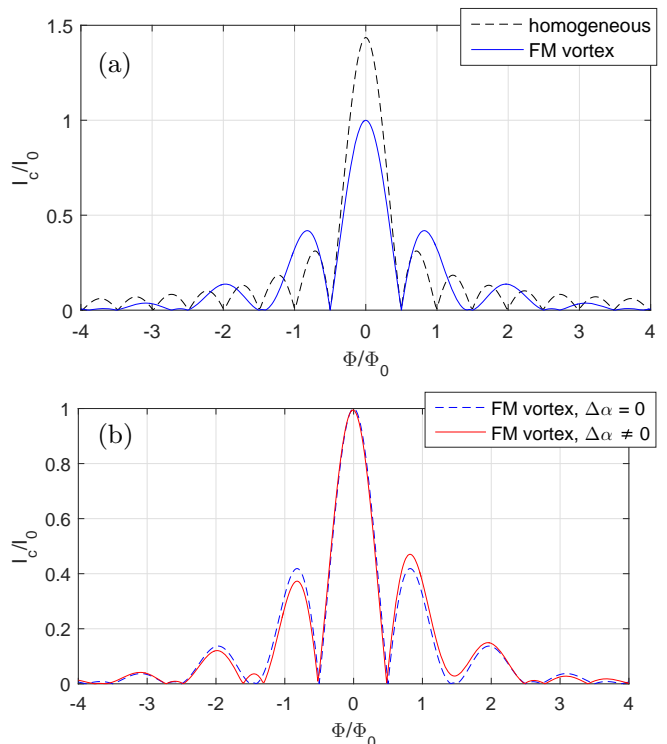


FIG. 2. (Color online) Interference patterns of the critical current as functions of the total magnetic flux through the junction $I_c = I_c(H)$. Upper panel: homogeneous junction (dashed curve) and in the presence of ferromagnetic (FM) vortex (solid curve) described by the $\theta(x)$ distribution (8). Lower panel: influence of the spin-dependent phase difference arising near the FM vortex core on the critical current. $\Delta\alpha = 0$ (dashed curve) and $\Delta\alpha(x) \neq 0$ given by the Eq. (9) (solid curve). Spin polarization is assumed to be such that $j_+ = 0.5j_-$ for all curves. The asymmetry of red solid curve $I_c(H) \neq I_c(-H)$ shows the presence of spontaneous superconducting currents.

imuthal angle of $\mathbf{h}_s = h_s(\cos \varphi_0, \sin \varphi_0, 0)$. Note that for $|m_z| = 1$ the superfluid velocity (7) is zero $\mathbf{V}_s = 0$. However this is not the case at $|m_z| < 1$. The effective phase difference can be found integrating the superfluid velocity across the junction $\Delta\alpha = \int_{-d}^d dy V_{Sy}$, where $2d$ is the junction width. For $\varphi_0 = 0$ and provided that $m_z \approx \text{const}$ at the scale $|y| < d$ one obtains in this way

$$\Delta\alpha(x) = 2[\arctan(m_z \tan \varphi) - m_z \varphi] \quad (9)$$

where $\varphi = \arctan(d/x)$.

The Josephson current can be calculated analytically assuming that the proximity effect is weak and one can use the linearized theory formulated for the component $f_\sigma = \text{Tr}[(\tau_x + i\tau_y)\hat{g}_\sigma]/2$. The linearized Usadel equation and expression for the current across the junction read

$$D_\sigma \hat{\nabla}^2 f_\sigma - 2\omega f_\sigma - \Delta_\sigma = 0 \quad (10)$$

$$\mathbf{j} = \pi T e \sum_{\sigma=\pm} \sum_{\omega} \nu_\sigma D_\sigma \text{Im}(f_\sigma \hat{\nabla} f_\sigma^*) \quad (11)$$

Since the distance between superconducting electrodes is small, proximity-induced vortices⁵⁰⁻⁵³ cannot form in the junction. Then the order parameter distribution can be approximated by the step-wise function

$$\Delta_\sigma(y) = h_\perp \Delta_{F\sigma} [\cos(\chi_\sigma/2) + i \text{Step}(y) \sin(\chi_\sigma/2)]. \quad (12)$$

It is convenient to choose the gauge so that $A_y = 0$ and neglect A_x component due to the small junction width. Then the total phase difference is given by $\chi_\sigma(x) = \Delta\chi + \sigma\Delta\alpha(x) + \phi x/L_J$, where $\Delta\chi = \chi_R - \chi_L$ and $\Delta\alpha(x) = \alpha_R - \alpha_L$ are the usual and spin-dependent phase differences, $\phi = \Phi/\Phi_0$ where Φ is the total magnetic flux through the junction area including the leads, Φ_0 is the flux quantum. The field \mathbf{Z} is treated as locally homogeneous and gauged it out by using the effective phase difference (9).

Within the above assumptions the linearized Usadel Eq.(10) can be solved analytically and Eq.(11) yields the following expression for the Josephson current density

$$j(x) = \sum_{\sigma=\pm} j_\sigma (\sin \theta)^2 \sin \chi_\sigma, \quad (13)$$

$$j_\sigma = \frac{\pi T e \nu_\sigma D_\sigma}{8} \sum_{\omega} \frac{\Delta_{F\sigma}^2}{\xi_{N\sigma} \omega^2}, \quad (14)$$

where $\xi_{N\sigma} = \sqrt{2|\omega|/D_\sigma}$. The total critical current is the given by $I_c = \sqrt{I_1^2 + I_2^2}$, where

$$I_1 = \sum_{\sigma} j_\sigma \int_{-L_J/2}^{L_J/2} (\sin \theta)^2 \cos(\phi x + \sigma \Delta\alpha) dx \quad (15)$$

$$I_2 = \sum_{\sigma} j_\sigma \int_{-L_J/2}^{L_J/2} (\sin \theta)^2 \sin(\phi x + \sigma \Delta\alpha) dx. \quad (16)$$

Fig.(2) presents the dependencies $I_c = I_c(\phi)$ calculated according to the Eqs.(15,16) with the help model distributions (8,9) for $\theta(x)$ and $\Delta\alpha(x)$, respectively. The upper panel shows the standard single-slit pattern from the homogeneous junction (dashed curve) and the double-slit pattern produced by the junction with FM vortex (solid curve). Here the spin-dependent phase is absent $\Delta\alpha = 0$. The distribution of $\theta(x)$ is taken in the form (8) with free parameters $w_{e,c}$. The homogeneous case is obtained in the limit $w_e, w_c \rightarrow 0$. Increasing the widths $w_{e,v}$ leads to the gradual transform of the interference pattern which at $w_e = w_c = 0.3$ acquires the double-slit form shown in the upper panel of the Fig.(2). Note that it is necessary to take into account the suppression of $\theta(x)$ both at the FM vortex core and at the boundary. In case when $w_e \rightarrow 0$ the interference pattern tends to the deformed homogeneous picture.

The spin-dependent phase $\Delta\alpha(x)$ can produce the Josephson current (13) even in the absence of the usual phase difference and external magnetic field. Since the phase shift has opposite signs in spin-up/down subbands the net effect on the current shows up only due to the certain amount of spin-filtering in the system^{34,35}, that

is $j_+ \neq j_-$. This is possible only if the spin-up and spin-down diffusion coefficients and/or DOS are different. The model distribution (9) produced by the FM vortex leads to the non-trivial modification of the Frahnhofer pattern, shown by the solid line in Fig.(2), lower panel. The parameters here are $d = 0.2L_J$, $j_- = 0.5j_+$. Asymmetric curve $I_c(H) \neq I_c(-H)$ is qualitatively similar to the one produced by the localized magnetic field or the internal phase shifts in junctions between chiral p -wave superconductors⁵⁴. Here the asymmetry is finite due to the spin filtering $j_+ \neq j_-$ and thus it signal the presence of spontaneous currents.

For the the S/F'/F setup with magnetic configurations similar to Fig.(1)a the effect of spontaneous current is rather tiny since the induced superfluid velocity is zero $\mathbf{V}_s = 0$ both at the center where $m_z = 0$ and outside the FM vortex core where $m_z = 1$. The situation becomes completely different for $\mathbf{z} \cdot \mathbf{h}_s \neq 0$. For example if $\mathbf{h}_s = h_s \mathbf{z}$ one can see that the spin-dependent phase is constant $\nabla\alpha = 0$ so that $\mathbf{V}_s = \sigma m_z \nabla\varphi/2$ and has singularity at $r = 0$. The current is however finite $j \sim h_\perp^2/r$ since $h_\perp = \sqrt{1 - m_z^2} \sim r$. This behaviour is similar to the orbital supercurrents around Abrikosov vortices in bulk superconductors. Note that this texture-induced spontaneous current is not related to the anomalous Josephson effect^{31-34,55-67} since it exists without the weak link in the superconducting layer. The singularity of \mathbf{Z} can be removed by the gauge transform introducing the vorticity to the spin-dependent phase $\alpha = \varphi$. Therefore in such system FM vortex generates singly-quantized superconducting vortices in the proximity-induced Berezinskii superconductor. The physics of such vortices and superconducting kinks that are generated by magnetic domain walls in the multilayer setups similar to the Fig.(1)a is potentially quite rich but is beyond the scope of the present paper.

To summarize, in this letter I explain the recent observation of the unusual magnetic field dependence of critical current of the Josephson junction through ferromagnetic vortex. The key theoretical finding is that the experimental results are consistent with the existence of proximity-induced Berezinskii superconductors in the S/F'/F systems with non-collinear strong ferromagnets. The effective order parameter amplitude is defined by the angle between magnetic moments in F and F' layers. The inhomogeneous distribution of this angle results in the double-slit interference pattern of the critical current. Besides that, the non-coplanar magnetic texture near the FM vortex core generates spin-dependent phase gradients and the emergent gauge field which can be combined into the invariant combination yielding the spin-dependent part of the superfluid velocity \mathbf{V}_s . The lifted degeneracy of DOS and diffusion coefficients in spin subbands in strong ferromagnets converts \mathbf{V}_s to the spontaneous supercurrent which is shown to result in the critical current asymmetry $I(H) \neq I(-H)$.

Finally, I show that FM vortex can induce spontaneous vorticity in the Berezinskii state, provided that

the magnetization in F' layer has an out-of-plane direction. That finding demonstrates that besides affecting transport properties of textured magnets^{41,68} the emergent gauge field can show up in the orbital motion of spin-triplet Cooper pairs and even produce topological defects in the superconducting order parameter. The re-

sult obtained here for the FM vortex are in general valid for magnetic skyrmions as well, owing to the similarity in their magnetization distributions.

I thank T. T. Heikkilä, A. Mel'nikov, I. Bobkova and A. Bobkov for stimulating discussions. The work was supported by the Academy of Finland.

-
- ¹ A. I. Buzdin, *Rev. Mod. Phys.* **77**, 935 (2005).
² F. S. Bergeret, A. F. Volkov, and K. B. Efetov, *Rev. Mod. Phys.* **77**, 1321 (2005).
³ M. Eschrig, *Reports on Progress in Physics* **78**, 104501 (2015).
⁴ J. Linder and J. W. A. Robinson, *Nat Phys* **11**, 307 (2015).
⁵ V. V. Ryazanov, V. A. Oboznov, A. Y. Rusanov, A. V. Veretennikov, A. A. Golubov, and J. Aarts, *Phys. Rev. Lett.* **86**, 2427 (2001).
⁶ S. M. Frolov, M. J. A. Stoutimore, T. A. Crane, D. J. Van Harlingen, V. A. Oboznov, V. V. Ryazanov, A. Ruosi, C. Granata, and M. Russo, *Nat Phys* **4**, 32 (2008).
⁷ A. K. Feofanov, V. A. Oboznov, V. V. Bol'ginov, J. Lisenfeld, S. Poletto, V. V. Ryazanov, A. N. Rossolenko, M. Khabipov, D. Balashov, A. B. Zorin, P. N. Dmitriev, V. P. Koshelets, and A. V. Ustinov, *Nat Phys* **6**, 593 (2010).
⁸ A. Iovan, T. Golod, and V. M. Krasnov, *Phys. Rev. B* **90**, 134514 (2014).
⁹ A. A. Golubov, M. Y. Kupriyanov, and Y. V. Fominov, *Journal of Experimental and Theoretical Physics Letters* **75**, 190 (2002).
¹⁰ J. W. A. Robinson, G. B. Halsz, A. I. Buzdin, and M. G. Blamire, *Phys. Rev. Lett.* **104**, 207001 (2010).
¹¹ J. W. A. Robinson, J. D. S. Witt, and M. G. Blamire, *Science* **329**, 59 (2010).
¹² M. S. Anwar, F. Czeschka, M. Hesselberth, M. Porcu, and J. Aarts, *Phys. Rev. B* **82**, 100501 (2010).
¹³ R. S. Keizer, S. T. B. Goennenwein, T. M. Klapwijk, G. Miao, G. Xiao, and A. Gupta, *Nature* **439**, 825 (2006).
¹⁴ L. R. Tagirov, *Phys. Rev. Lett.* **83**, 2058 (1999).
¹⁵ Y. V. Fominov, A. A. Golubov, and M. Y. Kupriyanov, *Journal of Experimental and Theoretical Physics Letters* **77**, 510 (2003).
¹⁶ V. I. Zdravkov, J. Kehrle, G. Obermeier, D. Lenk, H.-A. Krug von Nidda, C. Mller, M. Y. Kupriyanov, A. S. Sidorenko, S. Horn, R. Tidecks, and L. R. Tagirov, *Phys. Rev. B* **87**, 144507 (2013).
¹⁷ Y. V. Fominov, A. A. Golubov, T. Y. Karminskaya, M. Y. Kupriyanov, R. G. Deminov, and L. R. Tagirov, *JETP Letters* **91**, 308 (2010).
¹⁸ A. Singh, S. Voltan, K. Lahabi, and J. Aarts, *Phys. Rev. X* **5**, 021019 (2015).
¹⁹ M. Flokstra, J. M. van der Knaap, and J. Aarts, *Phys. Rev. B* **82**, 184523 (2010).
²⁰ M. A. Silaev, *Phys. Rev. B* **79**, 184505 (2009).
²¹ K. Lahabi, M. Amundsen, J. Ouassou, E. Beukers, M. Pleijster, J. Linder, P. Alkemade, and J. Aarts, *arXiv:1705.07020* (2017).
²² V. L. Berezinskii, *JETP Letters* **20**, 287 (1974).
²³ T. R. Kirkpatrick and D. Belitz, *Phys. Rev. Lett.* **66**, 1533 (1991).
²⁴ D. Belitz and T. R. Kirkpatrick, *Phys. Rev. B* **46**, 8393 (1992).
²⁵ D. Belitz and T. R. Kirkpatrick, *Phys. Rev. B* **60**, 3485 (1999).
²⁶ A. Balatsky and E. Abrahams, *Phys. Rev. B* **45**, 13125 (1992).
²⁷ E. Abrahams, A. Balatsky, D. J. Scalapino, and J. R. Schrieffer, *Phys. Rev. B* **52**, 1271 (1995).
²⁸ P. Coleman, E. Miranda, and A. Tsvetik, *Phys. Rev. B* **49**, 8955 (1994).
²⁹ Y. V. Fominov, Y. Tanaka, Y. Asano, and M. Eschrig, *Phys. Rev. B* **91**, 144514 (2015).
³⁰ I. V. Bobkova and Y. S. Barash, *Journal of Experimental and Theoretical Physics Letters* **80**, 494 (2004).
³¹ V. Braude and Y. V. Nazarov, *Phys. Rev. Lett.* **98**, 077003 (2007).
³² R. Grein, M. Eschrig, G. Metalidis, and G. Schn, *Phys. Rev. Lett.* **102**, 227005 (2009).
³³ S. Mironov and A. Buzdin, *Phys. Rev. B* **92**, 184506 (2015).
³⁴ M. A. Silaev, I. V. Tokatly, and F. S. Bergeret, *Phys. Rev. B* **95**, 184508 (2017).
³⁵ I. V. Bobkova, A. M. Bobkov, and M. A. Silaev, *arXiv:1706.04239* (2017).
³⁶ F. S. Bergeret, A. F. Volkov, and K. B. Efetov, *Phys. Rev. Lett.* **86**, 3140 (2001).
³⁷ F. S. Bergeret, A. Verso, and A. F. Volkov, *Phys. Rev. B* **86**, 214516 (2012).
³⁸ F. S. Bergeret, A. Verso, and A. F. Volkov, *Phys. Rev. B* **86**, 060506 (2012).
³⁹ N. B. Kopnin and A. S. Melnikov, *Phys. Rev. B* **84**, 064524 (2011).
⁴⁰ N. B. Kopnin, I. M. Khaymovich, and A. S. Melnikov, *Phys. Rev. Lett.* **110**, 027003 (2013).
⁴¹ G. E. Volovik, *Journal of Physics C: Solid State Physics* **20**, L83 (1987).
⁴² F. S. Bergeret, A. F. Volkov, and K. B. Efetov, *Phys. Rev. Lett.* **86**, 4096 (2001).
⁴³ Y. Tanaka and A. A. Golubov, *Phys. Rev. Lett.* **98**, 037003 (2007).
⁴⁴ Y. Tanaka, A. A. Golubov, S. Kashiwaya, and M. Ueda, *Phys. Rev. Lett.* **99**, 037005 (2007).
⁴⁵ Y. Tanaka, Y. Tanuma, and A. A. Golubov, *Phys. Rev. B* **76**, 054522 (2007).
⁴⁶ T. Yokoyama, *Phys. Rev. B* **86**, 075410 (2012).
⁴⁷ A. M. Black-Schaffer and A. V. Balatsky, *Phys. Rev. B* **86**, 144506 (2012).
⁴⁸ C. Triola and A. V. Balatsky, *Phys. Rev. B* **94**, 094518 (2016).
⁴⁹ T. Yokoyama, Y. Tanaka, and A. A. Golubov, *Phys. Rev. B* **75**, 134510 (2007).
⁵⁰ M. Alidoust, A. Zyuzin, and K. Halterman, *Phys. Rev. B* **95**, 045115 (2017).
⁵¹ J. C. Cuevas and F. S. Bergeret, *Phys. Rev. Lett.* **99**, 217002 (2007).

- ⁵² M. Alidoust and J. Linder, *Phys. Rev. B* **87**, 060503 (2013).
- ⁵³ M. Alidoust and K. Halterman, *Journal of Applied Physics* **117**, 123906 (2015).
- ⁵⁴ F. Kidwingira, J. D. Strand, D. J. Van Harlingen, and Y. Maeno, *Science* **314**, 1267 (2006).
- ⁵⁵ A. Buzdin, *Phys. Rev. Lett.* **101**, 107005 (2008).
- ⁵⁶ A. A. Reynoso, G. Usaj, C. A. Balseiro, D. Feinberg, and M. Avignon, *Phys. Rev. Lett.* **101**, 107001 (2008).
- ⁵⁷ A. Zazunov, R. Egger, T. Jonckheere, and T. Martin, *Phys. Rev. Lett.* **103**, 147004 (2009).
- ⁵⁸ J.-F. Liu and K. S. Chan, *Phys. Rev. B* **82**, 184533 (2010).
- ⁵⁹ A. Brunetti, A. Zazunov, A. Kundu, and R. Egger, *Phys. Rev. B* **88**, 144515 (2013).
- ⁶⁰ T. Yokoyama, M. Eto, and Y. V. Nazarov, *Phys. Rev. B* **89**, 195407 (2014).
- ⁶¹ I. Kulagina and J. Linder, *Phys. Rev. B* **90**, 054504 (2014).
- ⁶² K. N. Nesterov, M. Houzet, and J. S. Meyer, *Phys. Rev. B* **93**, 174502 (2016).
- ⁶³ F. Konschelle, I. V. Tokatly, and F. S. Bergeret, *Phys. Rev. B* **92**, 125443 (2015).
- ⁶⁴ A. Moor, A. F. Volkov, and K. B. Efetov, *Phys. Rev. B* **92**, 214510 (2015).
- ⁶⁵ A. Moor, A. F. Volkov, and K. B. Efetov, *Phys. Rev. B* **92**, 180506 (2015).
- ⁶⁶ I. V. Bobkova, A. M. Bobkov, A. A. Zyuzin, and M. Alidoust, *Phys. Rev. B* **94**, 134506 (2016).
- ⁶⁷ D. B. Szombati, S. Nadj-Perge, D. Car, S. R. Plissard, E. P. A. M. Bakkers, and L. P. Kouwenhoven, *Nat Phys* **12**, 568 (2016).
- ⁶⁸ N. Nagaosa and Y. Tokura, *Nat Nano* **8**, 899 (2013).